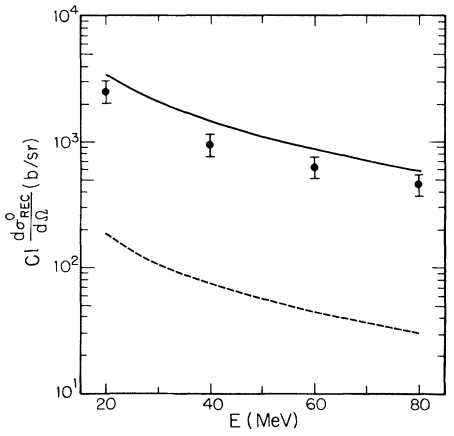

FIG. 4. Differential REC cross section per K vacancy at 90° to the incident beam vs Cl ion energy. The dashed curve was calculated from the Bethe-Salpeter (Ref. 13) free-electron capture theory, corrected for the $\sin^2\theta$ angular distribution of REC (Ref. 15). The solid curve was obtained by multiplying the free-electron theory by 19 which is the number of loosely bound (i.e., M- and N-shell) electrons in Cu.

formed.

This work was supported by the U. S. Energy Research and Development Administration.

[a]Present address: Department of Physics, East Carolina University, Greenville, N. C. 27834.

[1]H. W. Schnopper, H. D. Betz, J. P. Delvaille, K. Kalata, A. R. Sohval, K. W. Jones, and H. E. Wegner, Phys. Rev. Lett. 29, 898 (1972).

[2]R. Schulé, H. Schmidt-Böcking, and I. Tserruya, J. Phys. B 10, 889 (1977).

[3]J. Lindskog, J. Phil, R. Sjödin, A. Marelius, K. Sharma, R. Hallin, and P. Lindner, Phys. Scr. 14, 100 (1976).

[4]H. D. Betz, F. Bell, H. Panke, G. Kalkoffen, M. Welz, and D. Evers, Phys. Rev. Lett. 33, 807 (1974).

[5]F. Hopkins, Phys. Rev. Lett. 35, 270 (1975).

[6]T. J. Gray, P. Richard, K. A. Jamison, and J. M. Hall, Phys. Rev. A 14, 1333 (1976).

[7]J. A. Tanis and S. M. Shafroth, in Proceedings of the Seventh International Conference on Atomic Collisions in Solids, Moscow, 1977 (unpublished), and to be published.

[8]J. A. Tanis, S. M. Shafroth, T. Ainsworth, and J. Willis, Bull. Am. Phys. Soc. 22, 1314 (1977); J. A. Tanis, W. W. Jacobs, and S. M. Shafroth, to be published.

[9]J. A. Tanis, W. W. Jacobs, and S. M. Shafroth, to be published.

[10]E. Strom and H. I. Israel, Nucl. Data Tables, Sect. A 7, 565 (1970).

[11]Measured x-ray production was compared with tabulated values of proton-induced x-ray cross sections such as those found in C. H. Rutledge and R. L. Watson, At. Data Nucl. Data Tables 12, 195 (1973).

[12]The total REC cross section is given by $\sigma_{REC} = (8\pi/3)d\sigma_{REC}{}^0(90°)/d\Omega$ [see H. D. Betz, F. Bell, H. Panke, and G. Kalkoffen, in *Proceedings of the Fourth International Conference on Atomic Physics. Abstracts of Contributed Papers, Heidelberg, Germany, 1974*, edited by J. Kowalski and H. G. Weber (Heidelberg Univ. Press, Heidelberg, Germany, 1974), pp. 670–673].

[13]H. A. Bethe and E. E. Salpeter, *Quantum Mechanics of One- and Two-Electron Atoms* (Academic, New York, 1957), pp. 320–322.

[14]P. Kienle, M. Kleber, B. Povh, R. M. Diamond, F. S. Stephens, E. Grosse, M. R. Maier, and D. Proetel, Phys. Rev. Lett. 31, 1099 (1973).

[15]Betz *et al.*, Ref. 12.

Studies of Spontaneous Magnetic Fields in Laser-Produced Plasmas by Faraday Rotation

J. A. Stamper, E. A. McLean, and B. H. Ripin
Naval Research Laboratory, Washington, D. C. 20375
(Received 6 March 1978)

An extensive study has been made of the large magnetic fields in the plasma near the focus of a high-irradiance Nd-laser beam. The dependence of the magnetic field on many experimental conditions is noted—particularly timing and the presence of a preformed plasma. The data were obtained with a Raman-shifted, three-channel Faraday-rotation diagnostic system.

We report in this Letter the first broad-scale study of the large magnetic fields produced in the focal region of a high-irradiance Nd laser incident on a solid target. The study utilized a Raman-shifted probing beam with a three-channel Faraday-rotation diagnostic system. The first Faraday-rotation measurements[1] (in which magnetic fields in the megagauss range were ob-

© 1978 The American Physical Society

served) were reported in 1975. It was recognized that these fields could (primarily through their effect on thermal transport) play an important role in the physics of laser fusion.[2,3] Recently, there has been considerable theoretical interest in these fields[4-7]—particularly in relation to resonant absorption. However, although several laboratories[8-12] have undertaken further Faraday-rotation studies, there has been no published confirmation. This has led to some doubt about the magnitude and importance of the fields. Thus, the studies reported here are of particular significance. These Faraday-rotation studies have given reliable results for a variety of experimental conditions (timing, target material and geometry, laser irradiance and polarization, focal position, and prepulse effect) and have provided insight into the experimental conditions required for observing the fields.

At high laser irradiance ($\sim 10^{16}$ W/cm^2), the second-harmonic emission (5320 Å) from plasmas produced by our Nd-glass laser was so intense that a second-harmonic probe beam could not be used successfully (as it was at lower irradiance) for Faraday-rotation studies. An analogous problem was also encountered at the third harmonic.[12,13] However, the present experimental arrangement (shown in Fig. 1) uses a nonharmonic wavelength (6329 Å) to overcome the emitted-light problem. This is obtained by Raman shifting the second-harmonic probe beam in an ethanol cell.

The Raman-shifted probing beam (pulse width ~50 psec) is optically delayed to allow variation of the relative timing between the probe pulse and the main laser pulse. The vertically polarized probing beam is concentrated into the interaction region with an $f/300$-aperture lens. A diffraction-limited, $f/2$ lens is used to collimate the probing beam which has passed through the plasma. The collimated beam is then split into three beams with a 5° quartz wedge. These beams are focused (with separate 2-m–focal-length lenses) and pass through three independently oriented polarization analyzers (plastic sheet polarizers) to provide three channels of information. Space-resolved images are recorded (at focus) on Polaroid film. Thus, experimental correlations are available among the three channels to rule out any effects due to density gradients or transverse magnetic fields.[14]

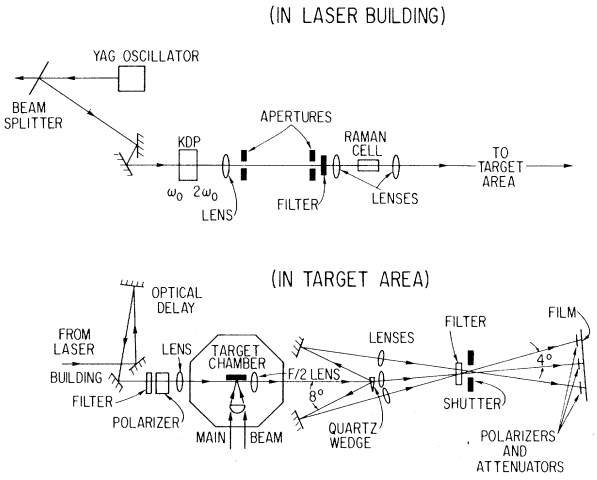

FIG. 1. Diagram of experimental arrangement.

The targets were irradiated with a beam from the NRL Pharos II Nd-laser system.[15] The output pulses (~5 J) with pulse duration of 75 psec (full width at half-maximum) were focused with an (aspheric) $f/2$ lens to a half-energy focal diameter of 25 μm, yielding an average irradiance of 10^{16} W/cm^2. Data were taken using polystyrene, $(CH)_n$, and steel (razor blade) slab targets and using polystyrene spherical targets.

Probe-beam timing was varied with respect to the peak of the main laser pulse. Faraday rotation of the probing light appeared (for the steel targets) as early as +15 psec, maximized near +50 psec, and then decreased (but could be seen as late as +450 psec). The dependence of the magnetic fields on timing was not strongly correlated with target material. The data presented here were all obtained at the +50-psec timing. Data were also taken with and without a prepulse on the incident laser beam and this, as shown later, proved to be an important effect. Laser irradiance was lowered by about an order of magnitude either by moving the focal position with respect to the target or by attenuating the laser beam energy. In both cases, the low-irradiance shots showed no observable Faraday rotation. However, a prepulse was not used and timing was not varied on the low-irradiance shots. All of the remaining data presented here were obtained with the target at good focus.

An attempt was made to observe the magnetic fields associated with resonant absorption.[5-7] Data were taken at early times (−15 to +15 psec) using a tilted (20°) iron target oriented so that the main laser beam was in either an s or p polarization state with respect to the density structure. No rotation was observed, perhaps indicating that the probe beam did not sample close

enough to the critical region.

The trend of variation of the Faraday-rotation data with target material, target geometry, and a laser prepulse is illustrated in Figs. 2 and 3. Each photograph shows the actual orientation of the target when looking into the probing beam with the main laser beam incident from the right. The orientation of each polarization analyzer (with respect to the incident polarization) is indicated (in degrees) under the photograph. The analyzer orientation and Faraday rotation angle are both taken, viewing into the probing beam, as positive when counterclockwise. The rotation angle for a given region on the photgraph can be estimated by comparing the exposure (varying as the square of the cosine of the angle between the beam polarization and the analyzer) at that region with that of the background.

Results for slab targets are shown in Fig. 2. The photographs in the top row are for a polystyrene target irradiated by a single 3.5-J laser pulse. Note the well-localized bright regions above or below center. These correspond to light that has been Faraday rotated to give locally enhanced transmission through the analyzer. The up-down asymmetry and its reversal with analyzer orientation are consistent with thermally generated magnetic fields[16,17]—oriented azimuthally about the laser-beam axis. Similar results were obtained for slab steel targets with a single laser pulse. A prepulse containing 3% of the total 4.4-J energy irradiated the same target 2 nsec ahead of the main pulse for the results shown in the second row. The presence of the preformed plasma due to the prepulse increased the intensity and spatial extent of the rotated light, without affecting the magnetic field orientation. A distinct darkening below the background level exists vertically opposite to the bright region. This, too, is consistent with azimuthally oriented magnetic fields since the rotated light in that region is closer to a cross-polarized state than is the background. The bottom row of photographs (in Fig. 2) is also a 3% prepulse case (of 6.5 J total) but using a steel (razor blade) target. Here, with both a prepulse and a target of higher atomic number, the Faraday rotation was most observable and had the largest spatial extent, but not necessarily the largest magnetic field.

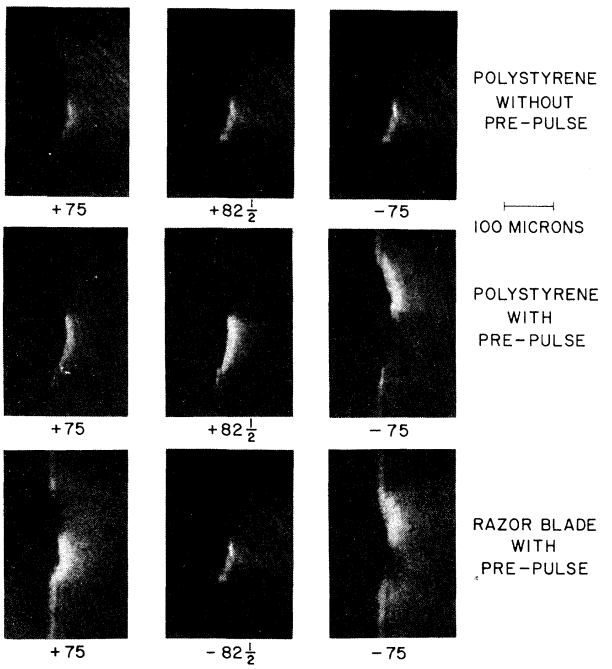

FIG. 2. Faraday-rotation photographs for slab targets, without and with prepulse. View is into probing beam with main laser beam incident from the right. Analyzer orientation (with respect to the incident polarization) is shown below each photograph. The position of rotated light (bright region) reverses with reversal of analyzer orientation. Probe-pulse timing was + 50 psec.

Earlier studies at NRL[18] showed that a prepulse could have a marked effect on both x-ray and fast-ion production. The rather dramatic effect of a prepulse on backscatter[19] could be understood in terms of its effect on the density gradient. It is possible that density modification by the prepulse, via the thermally generated magnetic fields and their effect on thermal transport, could account for the observed prepulse effect on x rays and fast ions.

Faraday-rotation results for single-sided ir-

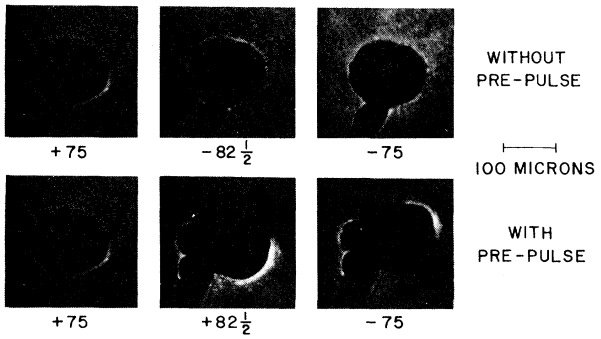

FIG. 3. Faraday-rotation photographs for spherical polystyrene targets, without and with prepulse. View, analyzer orientation, and timing are as in Fig. 2.

radiation of spherical polystyrene pellets are shown in Fig. 3. The top and bottom rows of photographs were taken on shots when the target was irradiated, respectively, with a 2-J (no prepulse) and 3.3-J (3% prepulse) main pulse. The pronounced effect of a prepulse is again present. Structure at the rear of the pellet on prepulse shots may have been due to some of the prepulse energy being transmitted through the polystyrene. The presumably unpolarized light there and in other parts of the photographs may be due to some depolarization of the probe beam (e.g., due to density gradients or magnetic fields[14]) or an intense plasma light emission. Note, that for the pellets as well as slabs, a reversal of the analyzer orientation always produces a corresponding reversal in the position of the bright region.

The direction of the magnetic field can be determined from the sense of Faraday rotation. The observed asymmetry is found to be consistent with the direction $\nabla T \times \nabla n$ of a thermally generated magnetic field, where ∇T is cylindrically in toward the laser axis, and ∇n is into the target; i.e., the magnetic field is clockwise when looking in the direction of the main laser beam. The azimuthal direction was unchanged throughout the observation interval (+15 to + 450 psec) and is consistent with theoretical calculations[17] including the thermal force term.

The magnitude of the Faraday rotation angle θ along a path z can be estimated [when $\omega_c/\omega \ll (\omega/\omega_p)^2 - 1$] from

$$d\theta/dz = \omega_p^2 \omega_{cz}/2\bar{n}\omega^2 c, \quad (1)$$

where ω_{cz} is the z component of the electron cyclotron frequency, $(\bar{n})^2 = 1 - (\omega_p/\omega)^2$, and ω_p and ω are, respectively, plasma and probe frequencies. For a given density profile and a reasonable model of the magnetic field variation, one can estimate the magnitude of the magnetic field by integrating Eq. (1) along the probe-beam path.

There were two experimental inputs to the density evaluation: interferometry and the extent of the dark region in the Faraday-rotation photographs. This dark region results from rays being refracted out of the solid angle of the collection optics. Density structure was determined by Abel inversion of interferograms[20] taken with an $f/4$ collector but with the same target and laser conditions as for the $f/2$ Faraday-rotation data. The density was modeled by a spherical variation $\exp[-(r - r_0)/L]$, where the density scale length L is extrapolated over a radial distance of 10–12 μm from the interferometry. The radius r_0 of the critical density is then determined by requiring that a ray having the observed radius s (of dark region) at the turning point will be refracted through an $f/2$ collection angle (~ 14°). The magnetic field is also assumed to vary exponentially[17] with radius but with a scale length that is computed (with this density structure) from the observed radial variation of the Faraday rotation angle.

For example, the data for shot No. 3662 onto a spherical pellet (shown in the lower half of Fig. 3) gave a Faraday rotation angle of 8° at a radius s of 80 μm and decreased to 2° at a radius of 100 μm. Interferometry showed that L was less than 40 μm which required that the sampled magnetic field (at the turning point) be greater than 0.4 MG. The magnetic field predicted by this model is 0.6 ± 0.1 MG when (as is likely) $L = 20 \pm 5$ μm. We estimate the overall accuracy to be better than a factor of 2.

Some guidance can be given concerning the experimental condictions required for detecting Faraday rotation. We have found that it is important to use a high-intensity, nonharmonic wavelength probe and to look at an optimum time after arrival of the main laser pulse. The presence of a prepulse greatly enhanced the observability of the magnetic fields. The best results were also obtained for a small but nonzero deviation from the cross-polarized analyzer orientation. In fact, good data were not obtained in our previous studies with a cross-polarized Wollaston prism analyzer. This may be due to the fact that maximum contrast is not obtained, for a slightly depolarized beam, at the precise cross-polarized orientation.

In summary, a study utilizing a three-channel Faraday-rotation diagnostic system has shown the dependence of thermally generated magnetic fields on a variety of experimental parameters. Correlations between the channels, completely consistent with these fields for all the 72 data shots, give a high level of confidence in the results.

The authors would like to acknowledge the valuable contributions from R. H. Lehmberg, S. E. Bodner, J. M. McMahon, T. H. DeRieux, and E. Turbyfill. This work was supported by the U. S. Department of Energy.

[1]J. A. Stamper and B. H. Ripin, Phys. Rev. Lett. 34, 138 (1975).

[2]B. H. Ripin *et al.*, Phys. Rev. Lett. 34, 1313 (1975).
[3]R. A. Haas *et al.*, Phys. Fluids 20, 322 (1977).
[4]J. A. Stamper and D. A. Tidman, Phys. Fluids 16, 2024 (1973); J. A. Stamper, Phys. Fluids 19, 758 (1976).
[5]J. J. Thomson *et al.*, Phys. Rev. Lett. 35, 663 (1975).
[6]B. Bezzerides *et al.*, Phys. Rev. Lett. 38, 495 (1977).
[7]Wee Woo and J. S. DeGroot, Phys. Fluids 21, 124 (1978).
[8]H. Kuroda, in *Proceedings of the Conference on Laser Engineering and Applications, Washington, D. C., 1977* (IEEE, New York, 1977).
[9]V. V. Aleksandrov, private communication.
[10]D. T. Attwood, in *Proceedings of the Twelfth International Congress on High Speed Photography, Toronto, 1976* (Society of Photo-Optical Instrumentation Engineers, Redondo Beach, Calif., 1976), Vol. 97, p. 413. Later studies (private communication) at 100 psec and 10^{15} W/cm^2 for $\lambda = 2660$ Å showed no fields larger than 100 kG.
[11]D. V. Giovanielli, private communication.
[12]J. A. Stamper *et al.*, in Naval Research Laboratory (NRL) Memorandum Report No. 3591, 1977 (unpublished), p. 63.
[13]E. A. McLean *et al.*, Appl. Phys. Lett. 31, 825 (1977).
[14]R. H. Lehmberg and J. A. Stamper, NRL Memorandum Report No. 3703, 1978 (to be published).
[15]J. M. McMahon *et al.*, in NRL Memorandum Report No. 3591, 1977 (unpublished), p. 3.
[16]J. A. Stamper *et al.*, Phys. Rev. Lett. 26, 1012 (1971).
[17]D. G. Colombant and N. K. Winsor, Phys. Rev. Lett. 38, 697 (1977).
[18]B. H. Ripin, NRL Memorandum Report No. 3684, 1977 (unpublished).
[19]B. H. Ripin *et al.*, Phys. Rev. Lett. 39, 611 (1977).
[20]E. A. McLean *et al.*, to be published.

Laser-Induced Desorption of Impurities from the Macrotor Tokamak Walls

F. Schwirzke
Department of Physics and Chemistry, Naval Postgraduate School, Monterey, California 93940

and

Lena Oren, S. Talmadge, and R. J. Taylor
Center for Plasma Physics and Fusion Engineering, University of California, Los Angeles, California 90024
(Received 22 November 1977)

Flash heating by a laser pulse has been used to desorb loosely bound species from a spot on the tokamak wall. Spectral analysis of the suddenly increased impurity radiation from the plasma in front of the laser-heated spot gives information on the species and the amount of impurity atoms present on the surface at a specific point in time of the tokamak discharge. Loosely bound chromium has been found on the stainless-steel surface.

Since adequate plasma confinement and heating seem possible, impurity evolution and control are recognized now as being critical remaining obstacles on the way to magnetic fusion energy. Too high impurity concentrations adversely influence almost every aspect of plasma behavior in tokamaks. Usually a large fraction of the Ohmic power input is lost from the plasma by impurity radiation.[1] Oxygen and carbon are the main low-Z impurities in present-day tokamaks. Contamination of the plasma by these loosely bound species can be reduced by proper methods of discharge cleaning.[2] High-Z impurities like chromium, iron, nickel, etc., are also of great concern, particularly since they are present in the plasma at much higher density than expected from theory. No *in situ* surface preparation techniques exist today for their reduction.

In situ surface analysis of the impurities on the walls just before and during the tokamak discharge is most important for a better understanding of processes related to plasma-wall interactions, discharge cleaning, recycling, and impurity transport. Laser-induced desorption of loosely bound species[3] combined with time-resolved spectral analysis of impurity radiation were used in this experiment to demonstrate a new powerful method for *in situ* surface analysis under realistic conditions, i.e., at any time during the discharge.

An unfocused "low-power" laser pulse of 2.5–3 J, ~25 ns full width at half-maximum, from a K-1500 Korad ruby laser was directed through a window towards the inner wall of the Macrotor vacuum chamber, Fig. 1. A surface spot of about 10 cm^2 is flash heated by the absorbed laser radi-

© 19/8 The American Physical Society

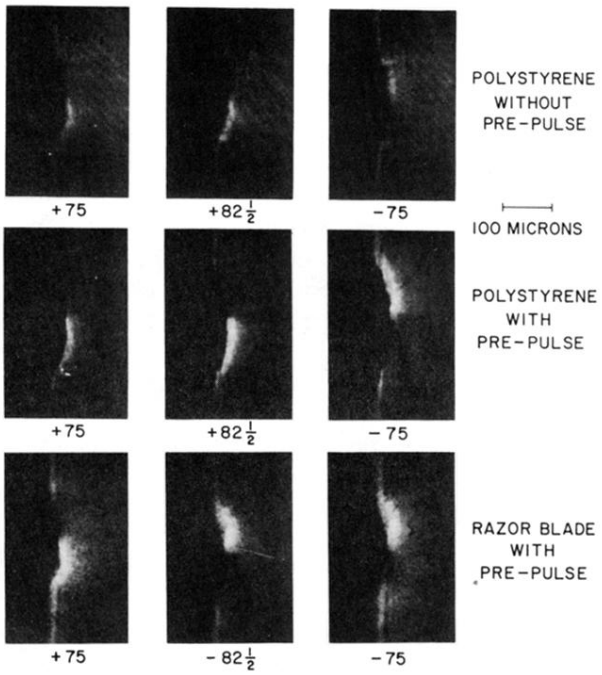

FIG. 2. Faraday-rotation photographs for slab targets, without and with prepulse. View is into probing beam with main laser beam incident from the right. Analyzer orientation (with respect to the incident polarization) is shown below each photograph. The position of rotated light (bright region) reverses with reversal of analyzer orientation. Probe-pulse timing was + 50 psec.

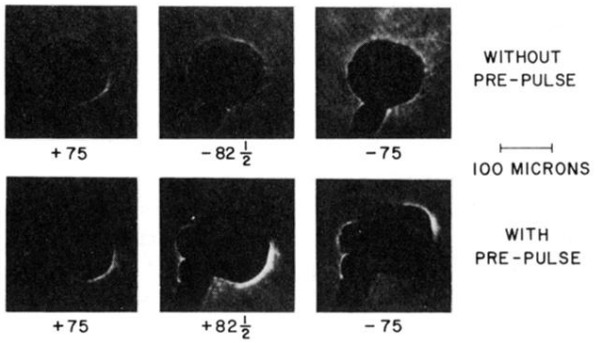

FIG. 3. Faraday-rotation photographs for spherical polystyrene targets, without and with prepulse. View, analyzer orientation, and timing are as in Fig. 2.